

# EFFECTIVE COLOR CORRECTION PIPELINE FOR A NOISY IMAGE

*Kenta Takahashi, Yusuke Monno, Masayuki Tanaka and Masatoshi Okutomi*

Tokyo Institute of Technology

## ABSTRACT

Color correction is an essential image processing operation that transforms a camera-dependent RGB color space to a standard color space, e.g., the XYZ or the sRGB color space. The color correction is typically performed by multiplying the camera RGB values by a color correction matrix, which often amplifies image noise. In this paper, we propose an effective color correction pipeline for a noisy image. The proposed pipeline consists of two parts; the color correction and denoising. In the color correction part, we utilize spatially varying color correction (SVCC) that adaptively calculates the color correction matrices for each local image block considering the noise effect. Although the SVCC can effectively suppress the noise amplification, the noise is still included in the color corrected image, where the noise levels spatially vary for each local block. In the denoising part, we propose an effective denoising framework for the color corrected image with spatially varying noise levels. Experimental results demonstrate that the proposed color correction pipeline outperforms existing algorithms for various noise levels.

*Index Terms*— Color correction, denoising, noise level

## 1. INTRODUCTION

In current color digital cameras, the spectral sensitivity of an image sensor usually differs from that of the human visual system. Therefore, a transformation of the camera-dependent RGB color space into a standard color space, typically the device-independent XYZ or the display sRGB color space, is required to improve color fidelity. This process is commonly called color correction. The color correction is one of the most essential and important operations in the digital color image processing pipeline.

In the past literatures, many algorithms have been proposed for the color correction including a least-square mapping with a linear model [1], a polynomial model [2], and a root-polynomial model [3], use of look-up tables [4], and a neural network approach [5]. Although these algorithms minimize the errors between the ideal and the color corrected values, they often amplify image noise. In practice, we need to take account of the noise for the color correction. A numerous number of denoising algorithms have also been proposed (see [6] for a review). To combine the color correc-

tion with the denoising, two straightforward approaches can be considered; (i) the denoising after the color correction and (ii) the color correction after the denoising. However, the simple combinations do not work well when the noise level (i.e., the standard deviation of the noise) is high, which will be shown in experimental results.

Several works addressed the suppression of the noise amplification by designing spectral sensitivity functions of the color filters [7–9] or developing a customized sensor without an IR-cut filter [10]. However, the spectral sensitivity functions are generally given and hard to manually design because of the requirement of hardware modifications. The development of the customized sensor is also expensive.

Some algorithms have also been proposed to suppress the noise amplification by the color correction [11–16]. In [11], the authors proposed a methodology for choosing an appropriate color correction matrix that minimizes either a mean color error or a mean variance caused by the noise. In [12], the authors used low-pass filters to prevent the noise amplification. In [13], the authors applied the color correction to only high-energy components in the DCT domain. In [14, 15], an optimal color correction matrix was estimated by a least-square analysis considering both the color accuracy and the noise effect. In [16], the authors proposed spatially varying color correction (SVCC) that divides the image into local blocks and estimates the optimal color correction matrices for each local block considering the noise effect. Although these algorithms can successively suppress the noise amplification, the noise is still included in the color corrected image because these algorithms do not explicitly incorporate denoising functionality.

In this paper, we propose an effective color correction pipeline for a noisy image. The proposed pipeline consists of two parts; the SVCC and the denoising. As mentioned above, the SVCC is an effective color correction algorithm considering the noise effect. However, it is not straightforward to combine the SVCC with an existing high-performance denoising algorithm because the noise levels after the SVCC spatially vary for each local image block (see details in Sec. 2). Therefore, we propose an effective denoising framework for the noisy image with spatially varying noise levels. Experimental results demonstrate that the proposed color correction pipeline achieves clear improvements compared with existing algorithms.

## 2. SPATIALLY VARYING COLOR CORRECTION

In this section, we briefly review the SVCC [16] and a challenge for combining the SVCC with an existing denoising algorithm. First, let us consider a linear  $3 \times 3$  mapping for the color correction of a noise-free RGB image. The color correction by the linear mapping is described as

$$\mathbf{y} = \mathbf{M}\mathbf{x}, \quad (1)$$

where  $\mathbf{x}$  is the input noise-free RGB vector,  $\mathbf{y}$  is the color corrected RGB vector, and  $\mathbf{M}$  is the linear mapping matrix for the noise-free case. The linear mapping matrix  $\mathbf{M}$  is typically learned by a least-square manner based on training color samples.

In a practical situation, the input RGB image contains noise. In a noisy case, the linear mapping often amplifies the noise. To reduce the noise amplification, an optimal linear mapping matrix [14, 15] considering both the color accuracy and the noise effect is estimated as

$$\hat{\mathbf{M}} = \arg \min_{\mathbf{M}_n} E \left[ \|\mathbf{M}\mathbf{x} - \mathbf{M}_n\mathbf{x}_n\|^2 \right], \quad (2)$$

where  $\mathbf{x}_n = [r_n, g_n, b_n]^T$  is the noisy RGB vector,  $\mathbf{M}_n$  is the linear mapping matrix for the noisy case,  $E[\cdot]$  represents the expectation operator, and  $\hat{\mathbf{M}}$  is the estimated optimal linear mapping matrix that minimizes the expected value of the difference between the noise-free case and the noisy case.

In the following discussion, let us assume that the noise of each channel in the input RGB image is zero-means Gaussian noise with a spatially constant noise level. By assuming that the noise of each channel is independent of the noise-free RGB signals and independent of each other, the optimal linear mapping matrix can be estimated as

$$\hat{\mathbf{M}} = \mathbf{M}(\mathbf{C} - \mathbf{C}^n)^T (\mathbf{C}^{-1})^T, \quad (3)$$

where  $\mathbf{C}$  and  $\mathbf{C}^n$  are the correlation matrix of the noisy RGB vector and that of the noise, respectively. The correlation matrices are calculated as

$$\mathbf{C} = \begin{bmatrix} E[r_n^2] & E[r_n g_n] & E[r_n b_n] \\ E[r_n g_n] & E[g_n^2] & E[g_n b_n] \\ E[r_n b_n] & E[g_n b_n] & E[b_n^2] \end{bmatrix}, \quad (4)$$

$$\mathbf{C}^n = \text{diag}([\sigma_r^2, \sigma_g^2, \sigma_b^2]), \quad (5)$$

where  $[\sigma_r^2, \sigma_g^2, \sigma_b^2]$  is the noise variance of each channel, which is assumed to be known. In the SVCC [16], the input noisy RGB image is firstly divided into local image blocks. Then, optimal linear mapping matrices are estimated for each local block as shown in Fig. 1, where the correlation matrix  $\mathbf{C}$  is approximately estimated based on the input noisy values in each local block.

Although the SVCC can suppress the noise amplification, the noise still remains and needs to be removed. However, it is

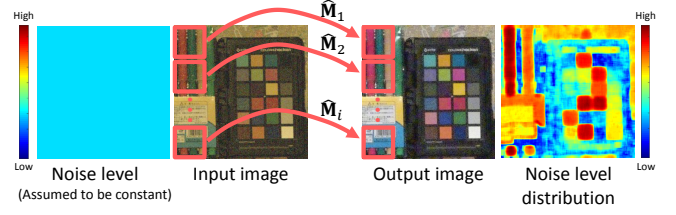


**Fig. 1.** Schematic illustration of the SVCC. The noise levels spatially vary after the SVCC.

not straightforward to combine the SVCC with denoising. In case the denoising is applied first, the denoising corrupts the assumption of the Gaussian noise, which is used in the SVCC. The case that the SVCC is applied first also has a challenge. As described before, the SVCC estimates the optimal linear mapping matrices for each local block. As a consequence, the noise levels after the SVCC spatially vary for each local block as shown in Fig. 1. However, most of existing denoising algorithms assume that the noise level is spatially constant for whole image pixels.

## 3. PROPOSED COLOR CORRECTION PIPELINE

Fig. 2 shows the proposed color correction pipeline for a noisy image. Given the camera-dependent noisy RGB image, our goal in this paper is to generate the display sRGB image while reducing the noise. We first apply the SVCC to correct the color of the noisy RGB image while suppressing the noise amplification. Then, we apply a denoising framework to the color corrected image with spatially varying noise levels after the SVCC.

In the following, we denote the noisy input image as  $\mathbf{X} = [\mathbf{x}_1, \mathbf{x}_2, \dots, \mathbf{x}_I]$ , where  $\mathbf{x}_i$  is the input noisy RGB vector at the pixel  $i$  and  $I$  is the number of pixels. We also denote the color corrected image as  $\mathbf{Y} = [\mathbf{y}_1, \mathbf{y}_2, \dots, \mathbf{y}_I]$ , where  $\mathbf{y}_i$  is the color corrected RGB vector. Based on the SVCC described in the previous section, we divide the input noisy image into  $k \times k$  blocks by a sliding manner and estimate the optimal linear mapping matrices for each block. For each pixel  $i$ , the color corrected RGB vector  $\mathbf{y}_i$  is calculated as

$$\mathbf{y}_i = \hat{\mathbf{M}}_i \mathbf{x}_i, \quad (6)$$

where  $\hat{\mathbf{M}}_i$  is the estimated optimal linear mapping matrix for the block centered at the pixel  $i$ .

Next, we calculate the noise level distribution of each channel after the SVCC. In the following, we omit the pixel index  $i$  to simplify the notation. At each pixel, the noise level of the R channel after the SVCC is calculated as

$$\hat{\sigma}_r = \sqrt{\hat{m}_{11}^2 \sigma_r^2 + \hat{m}_{12}^2 \sigma_g^2 + \hat{m}_{13}^2 \sigma_b^2} \quad (7)$$

where  $[\sigma_r^2, \sigma_g^2, \sigma_b^2]$  is the noise variance of the input noisy RGB image, which is assumed to be spatially constant and

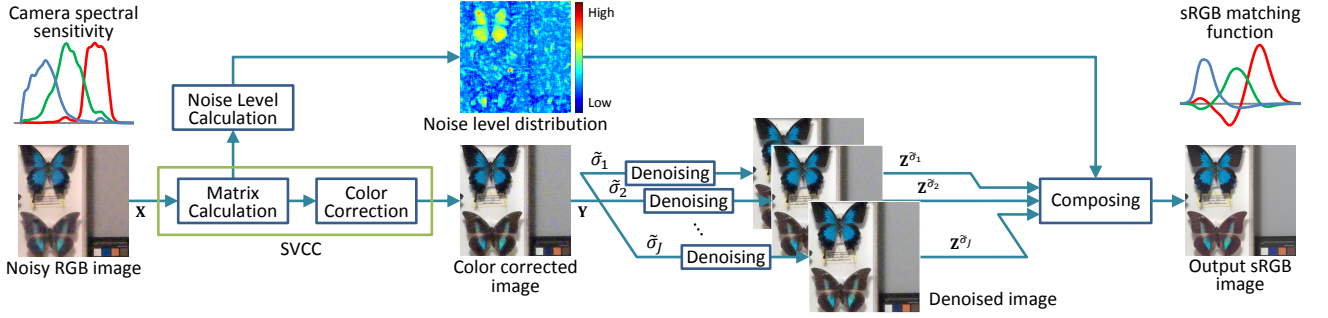


Fig. 2. Overall flow of the proposed color correction pipeline.

known,  $[\hat{m}_{11}, \hat{m}_{12}, \hat{m}_{13}]$  is the first row of the optimal linear mapping matrix  $\hat{\mathbf{M}}$ , which corresponds the coefficients for the R channel, and  $\hat{\sigma}_r$  is the calculated noise level at the pixel. Fig. 1 shows an example of the calculated noise level distribution for the R channel. The noise level distributions of the G and the B channels are calculated in the same manner.

Then, we apply a denoising framework to the color corrected image with the spatially varying noise levels. We first apply an existing high-performance denoising algorithm using preset assumed noise levels  $[\tilde{\sigma}_1, \tilde{\sigma}_2, \dots, \tilde{\sigma}_J]$ , where  $\tilde{\sigma}_1 < \tilde{\sigma}_2 < \dots < \tilde{\sigma}_J$  and  $J$  is the number of assumed noise levels. Each denoised image is expressed as

$$\mathbf{Z}^{\tilde{\sigma}_j} = \text{Dn}(\mathbf{Y}, \tilde{\sigma}_j), \quad (8)$$

where  $\mathbf{Z}^{\tilde{\sigma}_j}$  is the denoised image assuming that the noise level is  $\tilde{\sigma}_j$ ,  $\mathbf{Y}$  is the input color corrected image by the SVCC, and  $\text{Dn}(\mathbf{Y}, \tilde{\sigma})$  represents the denoising operation, which performs the denoising in a channel by channel manner.

To generate the final output image, we then compose the denoised images in a similar manner to [17]. The final output value of the R channel at each pixel is calculated as

$$g^r = (1 - \alpha^r) z^{r, \tilde{\sigma}_j} + \alpha^r z^{r, \tilde{\sigma}_{j+1}} \quad \text{s.t.} \quad \tilde{\sigma}_j \leq \hat{\sigma}_r < \tilde{\sigma}_{j+1}, \quad (9)$$

where  $g^r$  is the final output value of the R channel,  $z^{r, \tilde{\sigma}_j}$  is the denoised R value assuming the noise level  $\tilde{\sigma}_j$ , and  $\alpha^r$  is the weight that is adaptively changed based on the calculated noise level distribution as

$$\alpha^r = \frac{\hat{\sigma}_r - \tilde{\sigma}_j}{\tilde{\sigma}_{j+1} - \tilde{\sigma}_j} \quad \text{s.t.} \quad \tilde{\sigma}_j \leq \hat{\sigma}_r < \tilde{\sigma}_{j+1}, \quad (10)$$

where  $\hat{\sigma}_r$  is the calculated spatially varying noise level. The final output values of the G and the B channels are calculated in the same manner.

#### 4. EXPERIMENTAL RESULTS

In experiments, we used our hyperspectral image dataset [18, 19] of 40 scenes with  $512 \times 512$  pixels to simulate the whole color correction pipeline. The hyperspectral image is acquired at every 10nm from 420nm to 720nm. The ground-truth sRGB image was generated from the hyperspectral

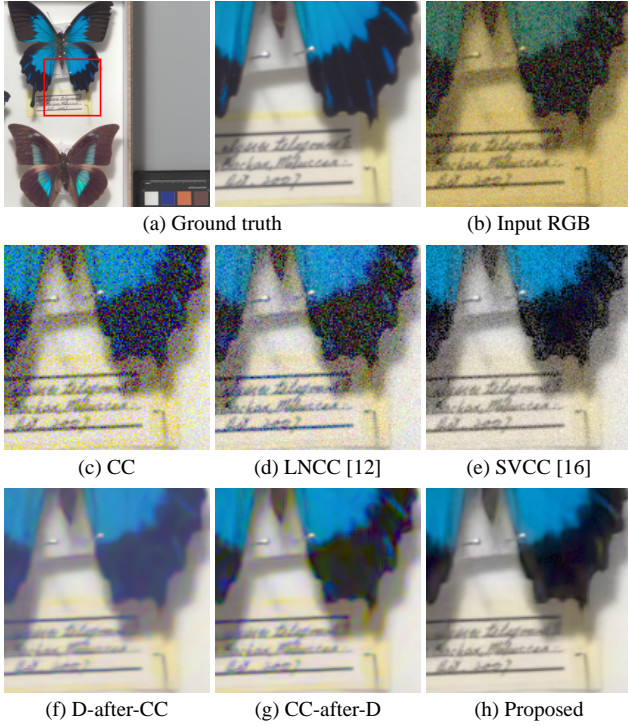
image by using color matching functions and the CIE D65 illumination with the correct white point. The camera RGB image was generated by assuming the Olympus E-PL2 camera sensitivity [20]. We evaluated the proposed pipeline for three illuminations; an incandescent light (CIE A), a daylight (CIE D65), and a fluorescent light (CIE F12). For each illumination, 20 scenes were used for training the color correction matrix and the other 20 scenes were used for testing the proposed pipeline. In the test stage, we added white Gaussian noise to the noise-free camera RGB image.

We compared the proposed pipeline<sup>1</sup> with five existing algorithms; (i) the color correction by the linear  $3 \times 3$  mapping (CC), (ii) the low noise color correction (LNCC) [12], (iii) the SVCC [16], (iv) the denoising after the color correction (D-after-CC), and (v) the color correction after the denoising (CC-after-D). The LNCC and the SVCC are color correction algorithms considering the noise effect. In the D-after-CC, the CC-after-D, and the proposed pipeline, we used the BM3D algorithm [21] for the denoising of each channel. In the proposed pipeline, we empirically used the  $21 \times 21$  blocks and set  $|\sigma_{j+1} - \sigma_j| = 2.5$  as the interval width of the assumed noise levels in Eq. (8).

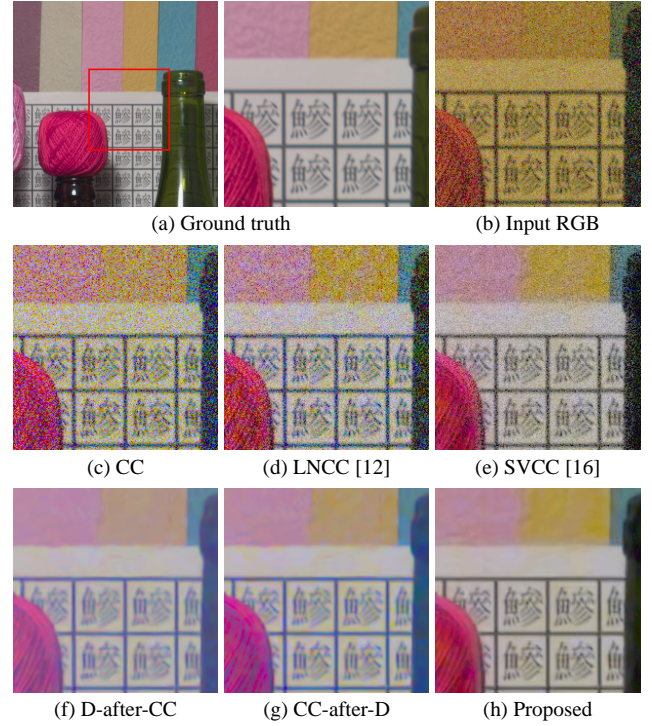
Fig. 3 shows the visual comparison of the result images for the CIE A illumination with the added noise level  $\sigma_r = \sigma_g = \sigma_b = 20$ . The proposed pipeline successfully reduce the noise without severe color artifacts in the wing of the butterfly. Fig. 4 shows the visual comparison for the CIE F12 illumination with the added noise level  $\sigma_r = \sigma_g = \sigma_b = 30$ . The proposed pipeline generates the visually pleasing image, while the other algorithms fail to remove the noise or generate severe color artifacts in the character region.

Table 1 and Fig. 5 show the average CPSNR performance of the test 20 images for different noise levels. Compared with the CC, the LNCC and the SVCC improves the performance because these algorithms take account of the noise effect. The D-after-CC and the CC-after-D reasonably work well for low noise levels. However, these algorithms yield poor results for high noise levels. In contrast, the proposed pipeline outperforms all algorithms and significantly improves the CPSNR performance especially when the noise level is high.

<sup>1</sup>Source code available: <http://www.ok.ctrl.titech.ac.jp/res/CC/CC.html>



**Fig. 3.** Visual comparison of result images (CIE A,  $\sigma = 20$ )



**Fig. 4.** Visual comparison of result images (CIE F12,  $\sigma = 30$ )

**Table 1.** Average CPSNR performance of 20 test images for different noise levels.

$\sigma$	A						D65						F12					
	5	10	15	20	25	30	5	10	15	20	25	30	5	10	15	20	25	30
CC	25.86	20.02	16.54	14.05	12.12	10.54	28.88	23.02	19.53	17.04	15.11	13.53	24.48	18.59	15.10	12.60	10.67	9.09
LNCC [12]	30.51	26.70	23.76	21.49	19.67	18.14	29.57	24.78	21.54	19.14	17.25	15.70	30.31	26.87	24.07	21.87	20.07	18.57
SVCC [16]	33.04	29.52	27.19	25.44	24.03	22.85	33.50	29.22	26.61	24.72	23.25	22.05	32.69	29.26	26.97	25.24	23.84	22.66
D-after-CC	35.16	31.23	28.05	25.56	23.55	21.94	36.82	33.31	30.65	28.48	26.66	25.12	34.48	30.03	26.65	24.03	22.07	20.60
CC-after-D	34.86	31.71	29.24	27.22	25.51	24.01	36.90	33.84	31.69	29.96	28.50	27.22	34.22	30.59	27.84	25.58	23.71	22.09
Proposed	<b>35.68</b>	<b>33.37</b>	<b>31.72</b>	<b>30.35</b>	<b>29.21</b>	<b>28.20</b>	<b>37.18</b>	<b>34.12</b>	<b>32.00</b>	<b>30.35</b>	<b>29.00</b>	<b>27.78</b>	<b>35.25</b>	<b>32.89</b>	<b>31.20</b>	<b>29.86</b>	<b>28.74</b>	<b>27.74</b>

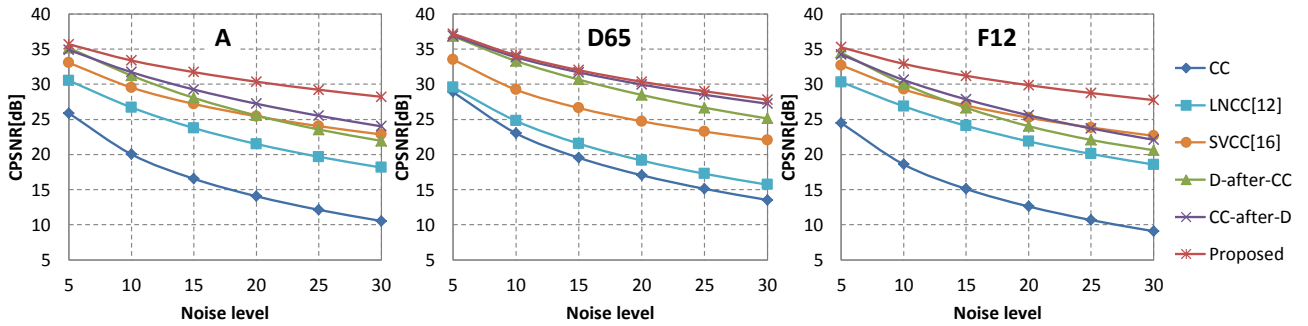


**Fig. 5.** Graphical presentation of average CPSNR performance of 20 test images for different noise levels.

## 5. CONCLUSION

In this paper, we have proposed an effective color correction pipeline for a noisy image. The proposed pipeline effectively incorporates the SVCC and the state-of-the-art denois-

ing algorithm. In particular, we have proposed a denoising framework for spatially varying noise levels derived from the SVCC. Experimental results demonstrate that the proposed pipeline achieves clear improvements compared with existing algorithms especially for high noise levels.

**Acknowledgment.** This work was partly supported by the MIC/SCOPE #141203024.

## 6. REFERENCES

- [1] H. R. Kang, *Computational color technology*, SPIE Press, 2006.
- [2] G. Hong, M. R. Luo, and P. A. Rhodes, "A study of digital camera colorimetric characterisation based on polynomial modelling," *Color Research and Application*, vol. 26, no. 1, pp. 76–84, 2001.
- [3] G. D. Finlayson, M. Mackiewicz, and A. Hurlbert, "Colour correction using root-polynomial regression," *IEEE Trans. on Image Processing*, vol. 24, no. 5, pp. 1460–1470, 2015.
- [4] P. C. Hung, "Colorimetric calibration in electronic imaging devices using a look-up-table model and interpolations," *Journal of Electronic Imaging*, vol. 2, no. 1, pp. 53–61, 1993.
- [5] H. R. Kang and P. G. Anderson, "Neural network applications to the color scanner and printer calibrations," *Journal of Electronic Imaging*, vol. 1, no. 2, pp. 125–135, 1992.
- [6] L. Shao, R. Yan, X. Li, and Y. Liu, "From heuristic optimization to dictionary learning: A review and comprehensive comparison of image denoising algorithms," *IEEE Trans. on Cybernetics*, vol. 44, no. 7, pp. 1001–1013, 2014.
- [7] M. J. Vrhel and H. J. Trussell, "Optimal color filters in the presence of noise," *IEEE Trans. on Image Processing*, vol. 4, no. 6, pp. 814–823, 1995.
- [8] P. Vora and C. Herley, "Trade-offs between color saturation and noise sensitivity in image sensors," *Proc. of IEEE Int. Conf. on Image Processing (ICIP)*, pp. 196–200, 1998.
- [9] N. Shimano, "Suppression of noise effects in color correction by spectral sensitivities of image sensors," *Optical Review*, vol. 9, no. 2, pp. 81–88, 2002.
- [10] B. K. Park and K.-H. Bae, "Color distortion correction without noise boost using multi-resolution analysis," *Proc. of IEEE Int. Conf. on Image Processing (ICIP)*, pp. 650–654, 2014.
- [11] U. Barnhöfer, J. DiCarlo, B. Olding, and B. Wandell, "Color estimation error trade-offs," *Proc. of SPIE*, vol. 5017, pp. 263–273, 2003.
- [12] L. Kharitonenko, S. Twelves, and C. Weerasinghe, "Suppression of noise amplification during colour correction," *IEEE Trans. on Consumer Electronics*, vol. 48, no. 2, pp. 229–233, 2002.
- [13] I. Kharitonenko and W. Li, "Image color correction in DCT domain," *Proc. of IEEE Int. Conf. on Consumer Electronics (ICCE)*, pp. 245–248, 2013.
- [14] Y.-P. Tan and T. Acharya, "A method for color correction with noise consideration," *Proc. of SPIE*, vol. 3963, pp. 329–337, 2000.
- [15] S. Quan, "Analytical approach to the optimal linear matrix with comprehensive error metric," *Proc. of SPIE*, vol. 5292, pp. 243–253, 2004.
- [16] S. Lim and A. Silverstein, "Spatially varying color correction (SVCC) matrices for reduced noise," *Proc. of Color and Imaging Conference (CIC)*, pp. 76–81, 2004.
- [17] Z. Liu, M. Tanaka, and M. Okutomi, "Signal dependent noise removal from a single image," *Proc. of IEEE Int. Conf. on Image Processing (ICIP)*, pp. 2679–2683, 2014.
- [18] Y. Monno, T. Kitao, M. Tanaka, and M. Okutomi, "Optimal spectral sensitivity functions for a single-camera one-shot multispectral imaging system," *Proc. of IEEE Int. Conf. on Image Processing (ICIP)*, pp. 2137–2140, 2012.
- [19] Y. Monno, S. Kikuchi, M. Tanaka, and M. Okutomi, "A practical one-shot multispectral imaging system using a single image sensor," *IEEE Trans. on Image Processing*, vol. 24, no. 10, pp. 3048–3059, 2015.
- [20] J. Jiang, D. Liu, J. Gu, and S. Süsstrunk, "What is the space of spectral sensitivity functions for digital color cameras?," *Proc. of Workshop on Applications of Computer Vision (WACV)*, pp. 168–179, 2013.
- [21] K. Dabov, A. Foi, V. Katkovnik, and K. Egiazarian, "Image denoising by sparse 3-d transform-domain collaborative filtering," *IEEE Trans. on Image Processing*, vol. 16, no. 8, pp. 2080–2095, 2007.